

UNCLASSIFIED

AR-001-952

DEPARTMENT OF DEFENCE
DEFENCE SCIENCE AND TECHNOLOGY ORGANISATION
ELECTRONICS RESEARCH LABORATORY

TECHNICAL REPORT
ERL-0124-TR

STRESS IN POROUS THIN FILMS THROUGH ADSORPTION
OF POLAR MOLECULES

E.H. Hirsch

S U M M A R Y

Films of magnesium fluoride are found to be under large tensile stress following exposure to water vapour. It is shown that this stress, which varies reversibly in magnitude with the adsorption equilibrium, can be attributed to electrostatic dipole interaction between the adsorbed water molecules.

The effect is not confined to magnesium fluoride, but can occur in other materials of an appropriate porous structure. Its relevance to the stability of optical coatings is discussed, together with some other applications.

Approved for Public Release

POSTAL ADDRESS: Chief Superintendent, Electronics Research Laboratory,
Box 2151, G.P.O., Adelaide, South Australia, 5001.

UNCLASSIFIED

TABLE OF CONTENTS

	Page No.
1. INTRODUCTION	1
2. EXPERIMENTAL ARRANGEMENT AND OBSERVATIONS	1 - 3
3. THEORY OF THE ADSORPTION STRESS	3 - 9
4. CONCLUSION	10 - 11
5. ACKNOWLEDGEMENTS	11
REFERENCES	12

LIST OF FIGURES

1. Experimental arrangement (schematic)
2. Deflection of mica substrate as function of water vapour pressure
3. Effect of water vapour on a MgF_2 film covered by 500 Å of Ag
- 4(a). Model geometry - columnar film growth
- 4(b). Model geometry - two dipoles in circular cylindrical pore
5. Interaction integral I_0 as function of y_{max}
6. Dependence of $I(a, d_0)$ on molecular diameter d_0 and pore radius a
7. $\sqrt{\delta/p}$ as function of $1/\delta^3$
8. Mean adsorption energy as function of beam deflection
9. Effect of polar molecule adsorption on the refractive index of MgF_2

1. INTRODUCTION

In the course of an investigation into the stress behaviour of vacuum evaporated films it was observed that when freshly deposited layers of magnesium fluoride were exposed to the atmosphere, they immediately showed evidence of very substantial tensile stress. The phenomenon is not confined to MgF_2 films only, and in view of this more general importance, particularly in relation to the stability of optical coatings, it was decided to examine the effect in more detail. The purpose of this paper is to describe the experimental observations, and to propose a model for the mechanism leading to the production of the tensile stress.

2. EXPERIMENTAL ARRANGEMENT AND OBSERVATIONS

The experiments were made on MgF_2 films deposited onto thin mica substrates of 4 mm width, clamped at one end so as to form cantilevers of 20 mm free length, and stress measurements were carried out by the well known method of optically observing the deflection δ of the free end of the substrate(ref.1). With the usual simplifying assumptions inherent in this technique, and neglecting the Poisson ratio correction, the film stress per unit width is given by (ref.2):

$$S = \frac{4ED^2\delta}{3L^2T_f} \quad (1)$$

where E = Young's Modulus of the film

D = thickness of the substrate

L = length of cantilever

T_f = film thickness

Cleaved mica strips with thicknesses in the range from 0.016 mm to 0.025 mm were used as substrates. For each of these strips E was determined by observing the beam deflections produced by known weights, the measurements yielding an average value of 1.8×10^{10} kg/m², with little variation from sample to sample.

The film depositions and stress measurements were performed in the apparatus shown schematically in figure 1. A liquid nitrogen trapped oil diffusion pump permitted the experimental chamber to be evacuated to a base pressure of about 5×10^{-6} Torr, following which the system could be isolated from the pump by a baffle valve. Gas could then be admitted to any desired pressure p , measured on a membrane manometer. During this phase of the procedure condensible components of the filling gas, such as water vapour, could be removed from the experimental volume by means of a large, liquid nitrogen cooled freezing pocket.

The deflection of the cantilever was observed through a window, using an optical filar micrometer, capable of detecting movement down to about 0.01 mm.

For reasons of experimental convenience the MgF_2 films of about 4000 Å thickness were deposited with the vapour stream incident at an angle of roughly 45° to the substrate, which was at ambient temperature.

Earlier findings on MgF_2 films(ref.3,4) produced on glass or quartz substrates, have usually shown the films to possess an intrinsic tensile stress. In contrast to this, the present films, laid down on mica, were invariably under a compressive stress, typically of the order of 10^9 kg/m². The corresponding beam deflection remained quite stable as long as the film was kept in a good vacuum, but immediately after exposure to the atmosphere the strip began to move

in the direction opposite to its initial deflection. This response was rapid, and under suitable circumstances it continued well beyond the original "neutral" position, adopted by the strip prior to deposition of the film, thus indicating that a net tensile stress had been generated by exposure to the atmosphere.

The effect was reversible in the sense that when the experimental chamber was re-evacuated, the beam again took up the position corresponding to the intrinsic compressive stress found immediately after deposition, and moreover the sequence of air admission and evacuation could be cyclically repeated with good reproducibility. We conclude therefore that the original compressive stress remained preserved at a constant level throughout, but that superimposed on it was a variable tensile component, that, as we shall see below, depended in magnitude on the properties of the ambient atmosphere.

A series of experiments established unequivocally that admission of dry permanent gases such as oxygen, nitrogen, hydrogen or argon was, at pressures up to one atmosphere, quite ineffective in producing the tensile component of stress, but that the presence of water vapour, even at pressures well below one Torr, was sufficient to cause a readily observable tensile force, indicating that this was in fact the only atmospheric constituent to contribute significantly to the effect. Accordingly the subsequent work was focussed on determining the role played by H_2O . To this end moist laboratory air was introduced into the chamber at pressures of several hundred Torr, and, with the baffle valve closed, its water vapour component was condensed in the freezing pocket. After the system had reached stability, the liquid nitrogen was removed from the pocket, and the deflection of the beam was observed as a function of the changing pressure as the condensed water vapour was released into the chamber. Separate experiments confirmed that the beam position was not affected by stray thermal effects due to the presence or absence of the coolant.

The response of the system was greatly accelerated if, after condensation of the water vapour, the baffle valve was opened for a period long enough to evacuate the non-condensable gases from near atmospheric pressure to a level below 1×10^{-5} Torr, thus facilitating the subsequent diffusion of the vapour through the apparatus. This procedure, which left H_2O as the only significant constituent of the residual atmosphere, was considered the preferred experimental method, although the ultimate result of the observations was not affected by the presence of permanent gases at high partial pressure.

Observations on a number of films confirmed that the stress behaviour was very similar in all cases. As an example figures 2(a) and 2(b) summarise two typical experimental runs, both involving the same film, but with a different air filling used for each measuring sequence. The curves represent the beam deflection δ and the water vapour pressure p as functions of the time t , measured from the instant of removal of the coolant from the freezing pocket. Because of small, uncontrolled differences in the detailed manner in which liquid nitrogen was applied and withdrawn, the pressure-time dependence varied somewhat between runs. In particular figure 2(b) gives an example of a pressure overshoot that was occasionally noticed before dynamic adsorption-desorption equilibrium was established in the experimental chamber. It is seen that the resulting pressure maximum is associated with a corresponding maximum in the δ curve, demonstrating not only the reversible nature of the tensile stress, but also indicating roughly the speed with which the stress responds to pressure changes.

Although, as we have seen, the variations of δ and p with time are different in figures 2(a) and 2(b), a plot of δ versus p , using data from both runs, is the smooth curve of figure 2(c), proving the existence of a definite $\delta - p$ relation.

Since on the one hand H_2O appears to be the only atmospheric constituent involved, and since on the other hand the water molecule is also the only one amongst the various molecular species present to possess a permanent electric dipole moment, it seems reasonable to attempt an explanation of the tensile stress in terms of the mutual repulsion of molecular dipoles adsorbed on the walls of pores known to exist within the film. On this basis one would expect the generation of a tensile stress not to be a property specific to MgF_2 only,

but one that is shared by other substances with an appropriate porous structure, in particular by materials such as cryolite and ZnS that, in common with MgF_2 have columnar habits of growth. From the work of Pulker and Jung(ref.5), Kinoshita and Nishibori(ref.6) and Ogura et al(ref.7) it is known that these substances have pore structures that are readily penetrated by atmospheric moisture. The development of tensile stress has not yet been investigated in these other materials, but our work has shown that thin films of shellac* develop tensile stress in a similar manner, and of a magnitude comparable to that found in MgF_2 .

In contrast to this, vacuum deposited silver films do not exhibit the effect at all, although they are readily permeated by water vapour. This permeability can be demonstrated by depositing Ag onto a MgF_2 film and observing the deflection of the composite system on exposure to water vapour. Figure 3 shows the results of such an experiment, in which a 500 Å silver layer was put down on the same MgF_2 film that had been the subject of the earlier experiments relating to figure 2, and since preliminary measurements has established that the elastic properties of the arrangement were not significantly affected by the additional silver deposit, direct comparison of the data of figures 2 and 3 is possible. In forming the Ag film, care was taken to ensure that no portion of the MgF_2 was accessible to H_2O other than by penetration of the silver barrier, and bearing in mind that the latter on its own did not develop any tensile stress, the subsequent movement of the cantilever must be ascribed to water vapour that had passed through the barrier. In comparing this beam deflection with that shown in figure 2, it is evident that whilst the rate of pressure rise is similar in both cases, the high impedance offered by the silver film to the passage of H_2O leads to a far more sluggish response of the compound film, so that the equilibrium beam deflection is reached only about two hours after the steady state pressure level has been attained. It will also be noticed that, although this pressure level is higher than in the earlier experiment of figure 2, it results in a smaller ultimate deflection of the beam. We believe this may be due to some of the pores in the MgF_2 being blocked off by the silver film, and thus rendered inaccessible to the H_2O vapour.

The fact that any water vapour at all could penetrate to the MgF_2 clearly implies a degree of porosity in the silver layer, but to account for the absence of any detectable tensile stress when the latter on its own is exposed to moisture, we suggest that the number of pores per unit area of the Ag film may be too low. Alternatively the average pore diameter could be too small to accommodate the number of polar molecules required to produce a significant tensile force. This we shall discuss more fully in the next section, where we develop a simple model to describe how the tensile stress is related to the number of molecular dipoles adsorbed in the porous structure of the film.

3. THEORY OF THE ADSORPTION STRESS

In constructing a model for the stress mechanism we are not at this stage concerned with developing a theory of great numerical precision. Our aim is rather to establish whether or not an explanation in terms of dipole interactions between adsorbed molecules is at all feasible, i.e. whether, on the basis of such interactions, the observed tensile forces can be produced by realistic amounts of the adsorbate. In our particular case, involving water vapour at a pressure of a few Torr, adsorbed on a surface at ambient temperature, we take this to imply a surface coverage roughly in the range from one to ten monolayers.

Following Pulker and Jung (loc.cit.) we represent the columnar growth structure of the MgF_2 film by an aggregate of closely packed cylindrical columns

* Prepared by painting mica substrates with a solution of 1 g of shellac flakes in 15 cc of methyl alcohol.

of radius R (see figure 4(a)). In this model "pores" of cross-sectional area $(\sqrt{3} - \pi/2)R^2$ are formed between any three adjacent cylinders. To simplify the calculations, we replace the resulting rather complex pore shape by circularly cylindrical pores of radius a , chosen so as to yield the same cross-sectional area.

From simple geometrical considerations it is found that these "equivalent" pores have a radius:

$$a = \sqrt{\frac{\sqrt{3}}{\pi} - \frac{1}{2}} R = 0.23 R \quad (2)$$

and that the spacing between adjacent pore centres:

$$s = \frac{(\sqrt{3} - \frac{1}{\sqrt{3}})a}{\sqrt{\frac{\sqrt{3}}{\pi} - \frac{1}{2}}} \cong 10a \quad (3)$$

We now consider the adsorbed molecular dipoles to be arranged on the cylindrical pore wall with their axes arranged normal to the surface, and with charges of the same sign pointing inward and outward respectively. We shall take the circumference of the adsorbing surface to remain at the constant value of $2\pi a$, irrespective of the amount of material adsorbed, i.e. we disregard the decrease in area available for adsorption as the thickness of the adsorbate layer becomes appreciable.

Let the length of the pore be equal to the film thickness T_f , and let us introduce a cartesian co-ordinate system, the z -axis of which is coincident with the pore axis, whilst the x - and y -axes lie in the centre plane of the film, with the x -axis pointing along the length of the mica strip i.e. in the direction of the tensile stress (see figure 4(b)). A dipole of moment M_1 is aligned along the x -axis in the x - y plane, and we wish to examine its interaction with a second dipole of moment M_2 , arranged at a vertical height h above the centre plane and displaced azimuthally from M_1 by an angle ϕ . The force along vector \tilde{r} connecting M_1 and M_2 is given from elementary electrostatic theory (ref.8) as:

$$F_r = \frac{3M_1 M_2}{4\pi\epsilon |\tilde{r}|^4} (\sin\theta \sin\theta^1 \cos\psi - 2\cos\theta \cos\theta^1) \quad (4)$$

Here ϵ is the dielectric constant of free space, ψ is the angle between the planes intersecting in \tilde{r} that contain the dipole vectors M_1 and M_2 , whilst θ and θ^1 are the angles between \tilde{r} and the two dipole axes, as indicated in the figure.

Introducing the normalised vertical height:

$$y = \frac{h}{a} \quad (5)$$

it can readily be shown that:

$$\sin\theta = \frac{\sqrt{\sin^2\phi + y^2}}{\sqrt{(2\sin(\phi/2))^2 + \sin^2\phi + y^2}} \quad (6)$$

$$\sin\theta^1 = \sqrt{\frac{\sin^2\phi(4\sin^2(\phi/2)(\sin^2(\phi/2) + \cos\phi) + 1) - \sin^4\phi + y^2}{(2\sin^2(\phi/2))^2 + \sin^2\phi + y^2}} \quad (7)$$

$$\cos\theta = \frac{2\sin^2(\phi/2)}{\sqrt{(2\sin^2(\phi/2))^2 + \sin^2\phi + y^2}} \quad (8)$$

$$\cos^1 = \frac{2\sin^2(\phi/2)\cos\phi - \sin^2\phi}{\sqrt{(2\sin^2(\phi/2))^2 + \sin^2\phi + y^2}} \quad (9)$$

and

$$\cos\psi = \frac{y^2 \cos\phi + \sin^2\phi}{y^2 + \sin^2\phi} \quad (10)$$

In addition the absolute value of the vector \tilde{r} is given by:

$$|r| = a \sqrt{4\sin^2(\phi/2) + y^2} \quad (11)$$

Equations (6) to (11) express the various quantities appearing in equation (4) as functions of ϕ and of the normalised vertical height y . Therefore, making the appropriate substitutions, the interaction force acting along \tilde{r} is obtained in terms of these variables only. Multiplication by $\cos\theta$ yields $x_{M_1}^F$, the x- component of the interaction force on M_1 , which represents the contribution to the tensile force we are concerned with, and which from equations (4) and (6) to (11) may be written in the form:

$$x_{M_1}^F = \frac{3M_1 M_2}{4\pi\epsilon a^4} g(\phi, y) \quad (12)$$

where g is a function of ϕ and y only.

We require the tensile force on M_1 due not only to its interaction with M_2 , but due to that with all the polar molecules adsorbed on the pore wall. Rather than carrying out a summation over the entire set of discrete molecular dipoles, it is more convenient for the present to replace these by an equivalent continuous dipole layer of moment β per unit area, and to perform an integration, replacing M_1 and M_2 by dipole elements βdS_1 and βdS_2 of area dS_1 and dS_2 respectively. In our approximate calculation this procedure is permissible since, as shown by Topping(ref.9) the potential at a point in a dipole array is rather insensitive to a rearrangement of the individual dipoles, provided the change is made in a manner that leaves the average dipole moment per unit area constant.

Noting that:

$$dS_2 = a^2 d\phi dy$$

the total component of the tensile force on dM_1 then becomes:

$$\bar{F}_{M_1} = \frac{3\beta^2 dS_1}{4\pi\epsilon a^2} \int_{y_0}^{y_{\max}} \int_{\phi_0}^{\pi} g(\phi, y) d\phi dy = \frac{3\beta^2 dS_1}{4\pi\epsilon a^2} I \quad (14)$$

The value of the interaction integral I obviously depends on the integration limits of the variables ϕ and y , and it is these limits that need further consideration. The angular variable ϕ clearly has the upper limit π , and for a dipole element dM_1 on the midplane of the film y ranges up to $T_f/2$, but for an element not situated on this plane we assign a , for the moment, unspecified upper limit y_{\max} . Also, as a first step we take the lower limits ϕ_0 and y_0 to be both zero. Values of the integral I_0 computed on this basis are shown in the curve of figure 5 as a function of y_{\max} . It is seen that at $y_{\max} = 0.5 I_0$ has practically reached its asymptotic value of about 8.66. Since $h = ay$, this means that dipoles separated from dM_1 by a vertical distance h in excess of half a pore radius make only a small contribution to the interaction integral. In practice $T_f \gg a$, and we can therefore always set $y_{\max} = \infty$, irrespective of whether or not dM_1 lies in the midplane of the film. In doing so we introduce only an edge effect error, involving the small fraction of molecules adsorbed on the pore wall within a distance of less than $a/2$ from the film boundary.

By setting the lower limits ϕ_0 and y_0 equal to zero we are allowing the continuous dipole distribution to approach the axis of the dipole element dM_1 indefinitely closely. This leads to an overestimate of the interaction force, as in actual fact two neighbouring molecular dipoles are separated by a minimum distance d_0 , representing in our case the effective diameter of the water molecule. To obtain a better approximation we therefore restrict the closest approach to d_0 by setting $\phi_0 = d_0/a$ for $0 \leq y \leq d_0$ and $\phi_0 = 0$ for $y > d_0$.

Equation (14) then assumes the form:

$$\begin{aligned} \bar{F}_{M_1} &= \frac{3\beta^2 dS_1}{2\pi\epsilon a^2} \int_0^{d_0} \int_{d_0/a}^{\pi} g(\phi, y) d\phi dy + \int_{d_0}^{\infty} \int_0^{\pi} g(\phi, y) d\phi dy \\ &= \frac{3\beta^2 dS_1}{2\pi\epsilon a^2} I(a, d_0) \end{aligned} \quad (15)$$

where a factor 2 has been introduced to take into account the contribution from points both above and below the centre plane.

For a dipole element dM_1 not oriented along the x -axis, but inclined to it at an angle φ , the contribution to the tensile force acting on the film cross-section is obtained by multiplying equation (15) by $\cos\varphi$. For the entire pore wall one thus finds:

$$\bar{F}_{\text{pore}} = \frac{3\beta^2 I(a, d_0)}{\pi\epsilon a} \int_{-T_f/2}^{T_f/2} \int_{-\pi/2}^{\pi/2} \cos\varphi d\varphi dh = \frac{6\beta^2 T_f I(a, d_0)}{\pi\epsilon a} \quad (16)$$

Since there are $1/s \cong 1/10a$ pores per unit length (see equation (3)), the total tensile force acting on the cross-section of the film per unit width is given by:

$$F_{\text{total}} = \frac{6\beta^2 I(a, d_o) T_f}{10\pi\epsilon a^2} \quad (17)$$

Equating this to the total tensile force as derived from the observed beam deflection by means of equation (1) and solving for β one obtains for the dipole moment per unit area:

$$\beta = \frac{Da}{L} \sqrt{\frac{20 \pi \epsilon E \delta}{9 I(a, d_o) T_f}} \quad (18)$$

At this stage it is convenient to abandon the model of an equivalent continuous dipole layer, that we introduced earlier for ease of calculation, and instead regard β more realistically as being due to n dipoles per unit area, each having a dipole moment, a , so that:

$$\beta = na \quad (19)$$

and the number density of polar molecules adsorbed on the pore surface is obtained as:

$$n = \frac{Da}{aL} \sqrt{\frac{20 \pi \epsilon E \delta}{9 I(a, d_o) T_f}} \quad (20)$$

In order to evaluate this expression we must introduce appropriate numerical values for the effective molecular diameter d_o and for the pore radius a .

From the work of Pulker and Jung (loc.cit.) we expect the pore radius to lie roughly in the range from 10 Å to 20 Å, and the molecular diameter may be estimated from the area A covered by a molecule on the substrate, an area that we shall take to be circular. Following Dushman(ref.10) we write this area as:

$$A = \frac{4\sqrt{3}}{2} \left(\frac{M}{4\sqrt{2} N_a \rho} \right)^{2/3} \quad (21)$$

where N_a is Avogadro's number, whilst ρ and M are the density and molecular weight of the condensed adsorbate. The effective molecular diameter is then found as:

$$d_o = 1.4 \times 10^{-8} (M/\rho)^{1/3} \text{ cm} \quad (22)$$

yielding for H_2O a diameter of 3.6 Å. This represents an appropriate value only, but, as seen in figure 6(a), changes of the order of 10% to 20% in d_o do not affect the interaction integral $I(a, d_o)$ in a manner that would invalidate our analysis. Also, according to figure 6(b), for $d_o = 3.6$ Å

$$I(a, d_0) \cong 5.8 \times 10^8 a \quad (23)$$

where a is expressed in metres.

Equation (20) can therefore be written as:

$$n \cong 3.3 \times 10^{-10} \frac{D}{aL} \sqrt{\frac{Ea\delta}{T_f}} \quad \text{molecules/m}^2 \quad (24)$$

Introducing for our particular case:

$$\begin{aligned} \text{beam thickness } D &= 1.6 \times 10^{-5} \text{ m} \\ \text{beam length } L &= 2 \times 10^{-2} \text{ m} \\ \text{Young's Modulus } E &= 1.8 \times 10^{10} \text{ kg/m}^2 \\ \text{film thickness } T_f &= 4 \times 10^{-7} \text{ m} \\ \text{dipole moment } a &= 6.1 \times 10^{-30} \text{ M.K.S. units} \\ \text{pore radius } a &= 1 \times 10^{-9} \text{ m} \end{aligned}$$

we obtain:

$$n \cong 2.9 \times 10^{20} \sqrt{\delta} \quad \text{molecules/m}^2 \quad (25)$$

For $\delta = 5 \times 10^{-4} \text{ m}$ this yields $n \cong 6.5 \times 10^{18} \text{ molecules/m}^2$, representing roughly one monolayer, a value that probably underestimates n by a factor of order unity, an underestimate that arises at least in part from the fact that we have neglected any decrease in the dipole moment a due to mutual depolarisation of neighbouring molecules. In addition we have also selected a pore radius in the lower part of the expected range. Nevertheless the calculated value for n is of a reasonable order of magnitude (ref.11,12), thus confirming that an explanation of the tensile stress in terms of dipole interactions is feasible.

Equation (25) establishes a relation between n and the observed beam deflection δ . On the other hand, from general adsorption theory (ref.13) there is a further relation connecting n with the adsorption energy Q through the equation:

$$n = \frac{3.5 \times 10^{26}}{\sqrt{MT}} p \tau e^{Q/R_0 T} \quad \text{molecules/m}^2 \quad (26)$$

where R_0 is the gas constant (cal/mole), T the absolute temperature, and τ is the vibration period of the adsorbed particles, to which we assign the value of $1 \times 10^{-13} \text{ s}$ (de Boer, loc.cit. p35). In the above conventional form of the equation Q is regarded as a constant, an approach that is permissible when the adsorption takes place on a homogenous surface, and the surface coverage is sufficiently low to exclude interaction between the adsorbate molecules, but in our case it is more appropriate to replace Q by $\bar{Q}(n)$, a suitably weighted average value over all adsorbed molecules, and one that will in general vary with n . By equating expressions (25) and (26) we then find for $T = 300^\circ \text{K}$ that:

$$\frac{\sqrt{\delta}}{p} = 1.65 \times 10^{-9} e^{\bar{Q}(n)/600} \quad (27)$$

The ratio $\sqrt{\delta}/p$ can be derived from our experimental data (see figure 2), and as the graph of figure 7 shows, it may be satisfactorily represented over the range of our measurements by the empirical equation:

$$\frac{\sqrt{\delta}}{p} = \frac{9.9 \times 10^{-13}}{\delta^3} \quad (28)$$

where δ is expressed in metres and p in Torr. Substituting in equation (27) we obtain the average adsorption energy in terms of the beam deflection as:

$$\bar{Q}(n) = 600 \ln \left(\frac{5.4 \times 10^{-3}}{\delta^3} \right) \quad (29)$$

The solid portion of the curve in figure 8 represents the average adsorption energy calculated in this manner, but it must be realised that, because of its reliance on the empirical formula (equation (28)), equation (29) has only a limited range of applicability, particularly since our measurements of the dependence of δ on p extend only up to $\delta \cong 6 \times 10^{-4}$ m, and for beam deflections below about 2×10^{-4} m the data are only qualitative due to the limited accuracy of the manometer in the corresponding pressure range. This accounts for the fact that equation (29) predicts an unlimited rise of $\bar{Q}(n)$ as $\delta \rightarrow 0$, when in fact we must expect it to approach the adsorption energy for the bare adsorbent surface in the manner indicated qualitatively by the upper dotted portion of the curve. Similarly at large values of δ , when a number of adsorbate layers have been formed, $\bar{Q}(n)$ should gradually decrease to a value near the heat of vaporisation of water in the condensed phase ($\sim 10\,000$ cal/mole). This asymptotic value is seen to be quite compatible with the calculated curve of figure 8, although, in view of the various numerical uncertainties in our calculation, such a high degree of compatibility must to some extent be fortuitous. Nevertheless the fact that the calculated adsorption energies lie in the range expected from earlier experiments on water vapour adsorption (de Boer, loc.cit. p42), lends further credibility to our model.

As the total surface area A_p of the pore system within the film is covered by adsorbate molecules to a surface density n (in our example 6.5×10^{18} molecules/m²) an amount of energy:

$$H = \frac{n A_p \bar{Q}(n)}{N_a} \quad (30)$$

is released, and the question arises as to whether this energy is sufficient to account for the energy of elastic deformation stored in the cantilever. A simple calculation shows that under our conditions this energy is about 5×10^{-9} cal for a beam deflection of 5×10^{-4} m. The same value of δ yields from equation (29) an average adsorption energy $\bar{Q}(n)$ of 10 500 cal/mole. Also, with the aid of equation (3) the area of the pore system in a film of width W (in our case 4×10^{-3} m) is given by:

$$A_p = \frac{2\pi T_f W L \times 10^{-2}}{a} \quad (31)$$

so that for $a = 1 \times 10^{-9}$ m one obtains that $H = 2.3 \times 10^{-4}$ cal. The energy that becomes available during the adsorption process therefore exceeds the stored elastic energy by more than four orders of magnitude.

4. CONCLUSION

The results of the previous sections show that the tensile forces produced in a thin porous film by the adsorption of water vapour can be accounted for in terms of the electrostatic interaction of molecular dipoles, and according to our model polar molecules other than H_2O should cause similar effects. Moreover it is apparent from equations (17) and (23) that the forces due to the dipole interaction are approximately inversely proportional to the pore size, so that little stress will be found in films with very coarse porosity. The converse prediction of high stress when the pore size is small does however need some qualification, since our analysis assumes the thickness of the adsorbate to be small in comparison with the pore radius. This assumption will not in general hold for very fine pores, where moreover the number of adsorbed molecules will not only be determined by the dynamic equilibrium of adsorption (equation (26)) but an upper limit to this number will in addition be set by the amount of adsorbate that can be accommodated within the confines of the small pore volume. As a result, both very small and very large pores will lead to insignificant adsorption stress, but there is an intermediate range of pore radii, placed by our analysis roughly between 10 \AA and 100 \AA , where very substantial stresses (in our experiments of the order of $2 \times 10^7 \text{ kg/m}^2$) can be induced.

If this porosity range can be avoided by a suitable choice of film deposition parameters, there should not only be a considerable reduction in adsorption stress, but it would seem that also the optical stability of the films could be markedly improved. It has long been recognised that the refractive index n of MgF_2 films changes following exposure to atmospheric moisture. In the past this effect has been ascribed to water filling the voids within the film, and in doing so raising the refractive index of the pore space from 1.0 for air to 1.33 for H_2O , thus increasing the average refractive index of the film by an amount depending on the total pore volume. On the basis of this picture several authors have in fact deduced the film porosity from changes in the value of n .

On the other hand when a stress S is applied to a material, its refractive index can also be changed through the photo-elastic effect by an amount:

$$\Delta n = BS \quad (32)$$

where B is the appropriate stress-optical coefficient, measured in Brewsters, if S is expressed in dynes/cm² (ref.14). It is therefore of interest to examine whether the stress induced by H_2O adsorption could materially contribute by this mechanism to the observed variation in the refractive index.

A stress of about $2 \times 10^9 \text{ dyn/cm}^2$, as encountered in the present work, together with a typical refractive index change Δn of 5×10^{-3} (ref.6), would imply for B a value of 25 Brewsters. Whilst no photo-elastic data for MgF_2 appear to be available, $B = 25$ falls into a typical range for a number of materials (ref.14,15), thus making our hypothesis at least feasible.

We can obtain further supporting evidence from the manner in which n changes with the moisture content of the atmosphere. Since from equation (1) S is linearly related to the beam deflection δ , whilst according to equation (28) δ is in turn proportional to $p^{2/7}$, the photo-elastic change in n (equation (32)) can be expressed in terms of the partial pressure p of the water vapour as:

$$\Delta n = B_1 p^{2/7} \quad (33)$$

A variation in accordance with this power law is in fairly good agreement with experimental observations, as shown in figure 9(a), where data are reproduced, obtained by Kinoshita and Nishibori (ref.6) for a MgF_2 film exposed to an atmosphere of variable moisture content, the latter being expressed as a fraction of the saturated vapour pressure p_0 . The change in refractive index

is seen to be associated with hysteresis, and in the figure the solid curves are as drawn by the authors, whilst the dotted lines were calculated from an expression of the form of equation (33) with B_1 set equal to 7.3×10^{-3} . This value was arrived at by fitting the power law to the lower curve of figure 9(a), although acceptable agreement with the upper curve is also obtained, in spite of the fact that the latter, in view of the small number of experimental points given, is only semi-quantitative in nature.

The agreement of equation (33) with the experimental data of Kinoshita and Nishibori provides further support for our suggestion that adsorption induced stress may, via the photo-elastic effect, contribute substantially to the observed changes in the refractive index. Should this be the case, earlier estimates of film porosity based on variations in n (ref.6,7) may need reassessment.

It will however be noticed that significant departures from the $2/7$ power law occur for values of p/p_0 in excess of about 0.8. It is believed that these deviations may be due to the effect of capillary adsorption (de Boer, loc.cit. p210), and such an interpretation could also explain a similar departure in the same range of p/p_0 (see figure 9(b)), found by Kinoshita and Nishibori in the case of a MgF_2 film exposed not to H_2O but to ethyl alcohol vapour, a substance with a dipole moment comparable to that of water. The figure also shows that for p/p_0 below 0.8 the measurements are very convincingly represented by a $2/7$ power law, suggesting that our empirical equation (28), from which the power law is derived, is of greater generality than might initially have been expected. Thus the equation is seen to yield a good approximation for observations made on a number of films, prepared in different laboratories and exposed to different polar adsorbents. Particularly in view of this latter fact, it seems that the equation reflects a rather general trend in the manner in which the average adsorption energy $\bar{Q}(n)$ changes as the number of adsorbed molecules increases. Because of its fundamental implications this aspect will need further investigation.

Turning to some more immediately practical applications, the compound film technique (Ag/MgF_2) discussed in Section 2 affords a ready means of determining the penetration of H_2O , and presumably of other polar molecules, through thin films, provided the pore structure of these films is such as to prevent significant adsorption stress in the material, the permeability of which is under study.

On the other hand films of materials such as MgF_2 , that exhibit large adsorption stresses, constitute, in combination with a suitable elastic substrate, the sensing element of a simple and very sensitive hygrometer. Initial experiments point to a detection limit of such a device in the vicinity of 5×10^{-4} Torr partial pressure of H_2O ($\sim 3 \times 10^{-3}\%$ relative humidity), with good reproducibility up to pressures of several Torr, although there is some hysteresis when the elements are first exposed to very high water vapour pressures. This appears to be eliminated however by repeated cycling through the humidity range. The long term performance of such elements is now being investigated, and will be reported in due course.

5. ACKNOWLEDGEMENTS

The author wishes to express his appreciation to Mr I.K. Varga, who first drew his attention to the deformation of MgF_2 films following exposure to the atmosphere, and who made available the films used in the present investigation. Thanks are also due to Mr L.J. Dunne and Dr R.H. Hartley for helpful discussions, as well as to Mr B.A. Johnson for constructing the experimental apparatus and for his painstaking assistance with the measurements.

REFERENCES

No.	Author	Title
1	Chopra, K.L.	"Thin Film Phenomena". McGraw-Hill, New York, p269, 1969
2	Stoney, G.G.	Proc.Roy.Soc. (London) A, <u>82</u> , 172, 1909
3	Pulker, H.K., and Maeser, J.	Thin Solid Films, <u>59</u> , 65, 1979
4	Schroeder, H., and Schmidt, G.M.	Z.f. Angew.Physik, <u>18</u> , 124, 1964
5	Pulker, H.K., and Jung, E.	Thin Solid Films, <u>9</u> , 57, 1972
6	Kinosita, K., and Nishibori, M.	J.Vac.Sci. and Techn. <u>9</u> , 730, 1969
7	Ogura, S., Sugawara, N., and Hiraga, R.	Thin Solid Films, <u>30</u> , 3, 1975
8	Smythe, W.R.	"Static and Dynamic Electricity". McGraw-Hill, New York, 3rd Ed., p7, 1968
9	Topping, J.	Proc. Roy. Soc. (London) A, <u>114</u> , 67, 1927
10	Dushman, S.	"Scientific Foundations of Vacuum Technique". John Wiley & Sons Inc., New York, 2nd Ed., p420, 1962
11	Dushman, S.	"Scientific Foundations of Vacuum Technique". John Wiley & Sons Inc., New York, 2nd Ed., p448, 1962
12	Brunauer, S.	"The Adsorption of Gases and Vapours". Oxford University Press, p321, 1943
13	de Boer, J.H.	"The Dynamical Character of Adsorption". Oxford University Press, p45, 1953
14	Condon, E.U., and Odishaw, H.	"Handbook of Physics". McGraw-Hill, New York p6-121, 1958
15	Hendry, A.W.	"Photoelastic Analysis". Pergamon Press, London, p126, 1966

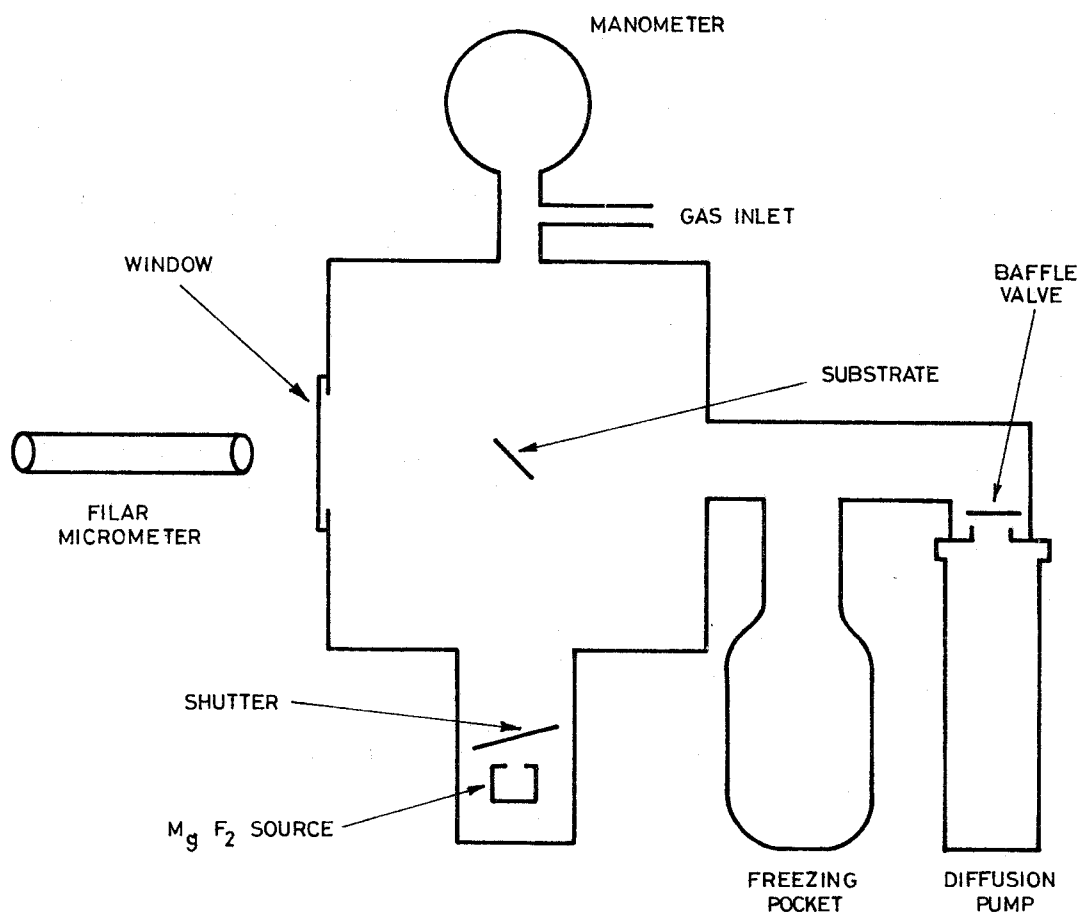
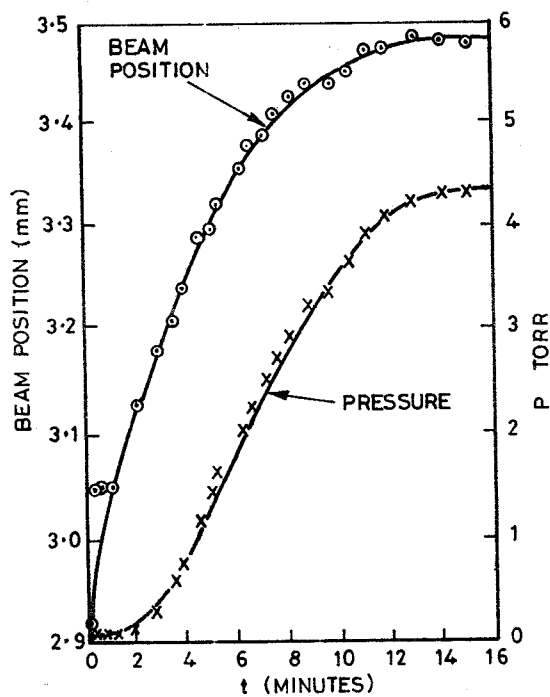
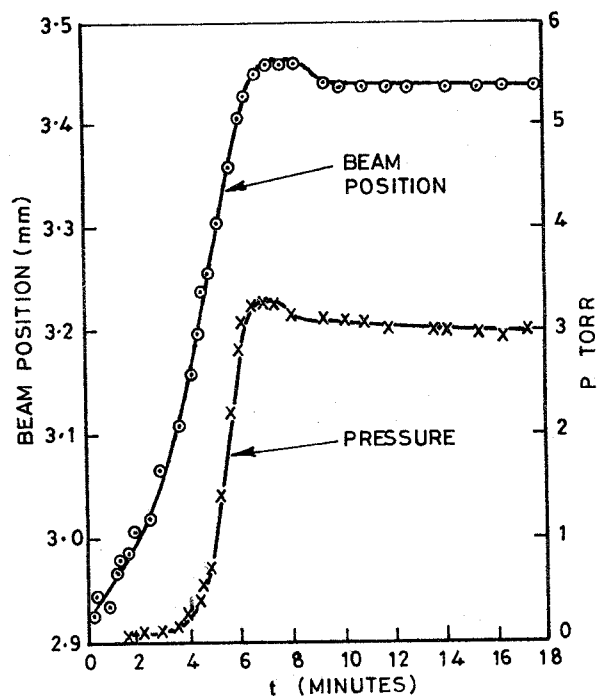


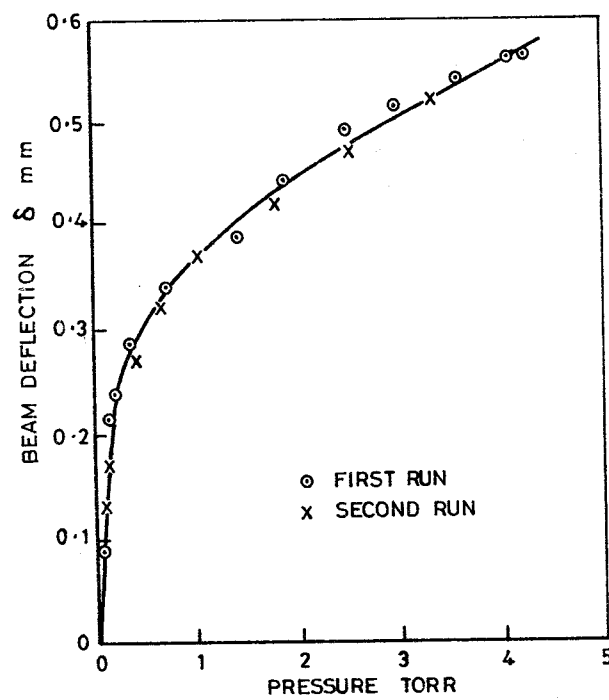
Figure 1. Experimental arrangement (schematic)



(a)



(b)



(c)

Figure 2. Deflection of mica substrate as a function of water vapour pressure

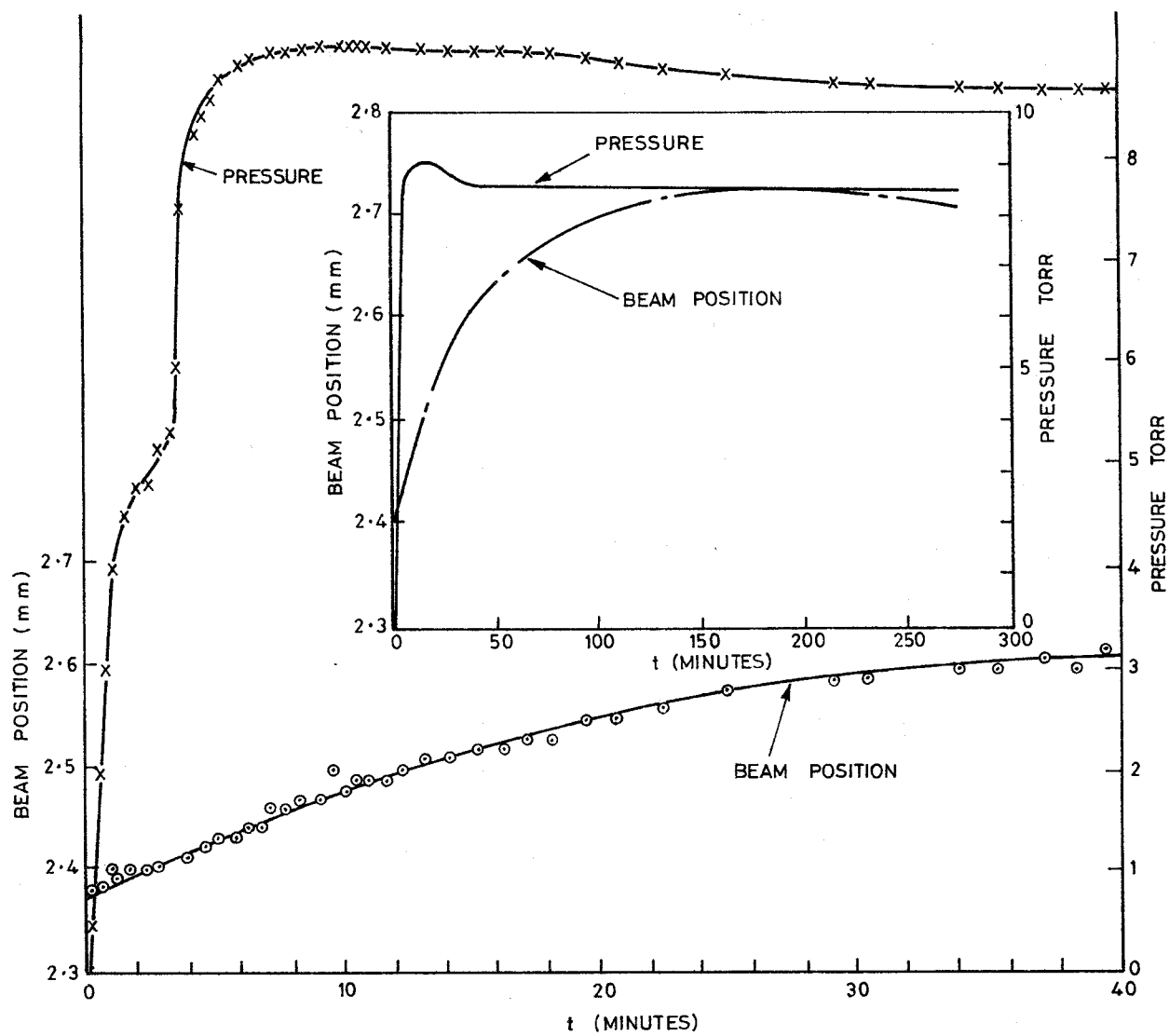


Figure 3. Effect of water vapour on a MgF_2 film covered by 500 Å of Ag

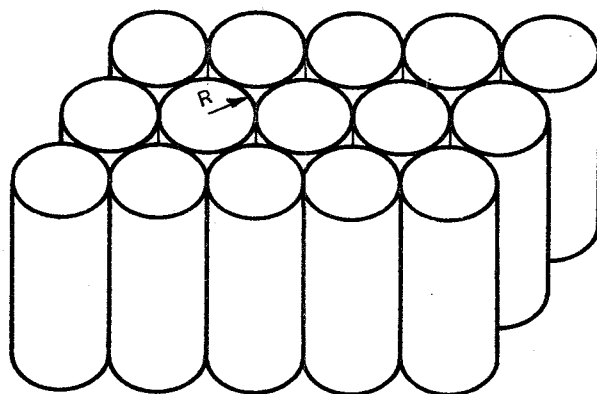


Figure 4(a). Model geometry - columnar film growth

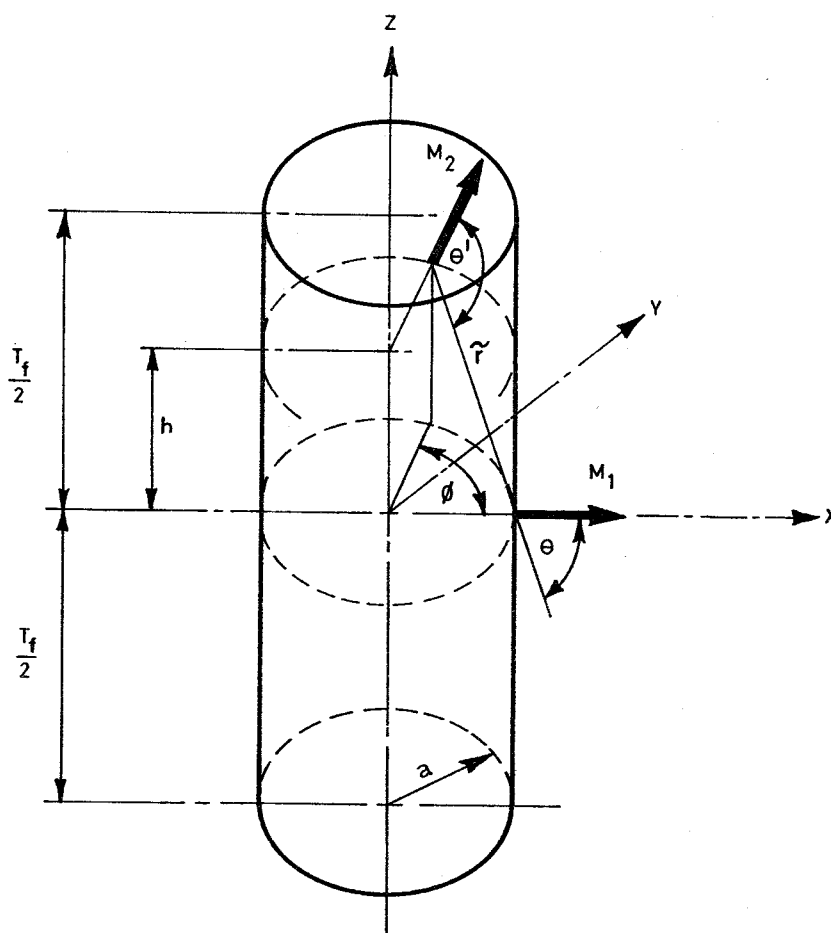


Figure 4(b). Model geometry - two dipoles in circular cylindrical pore

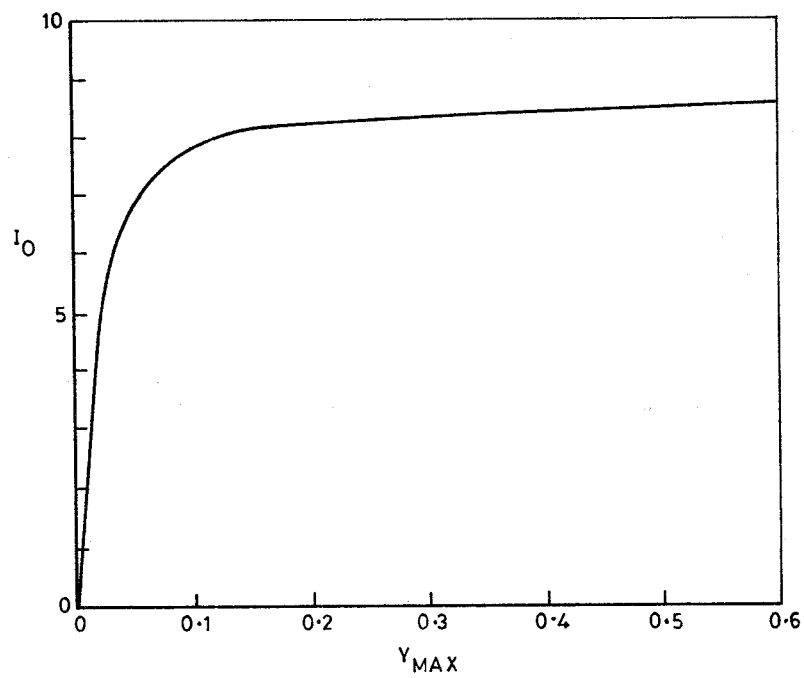
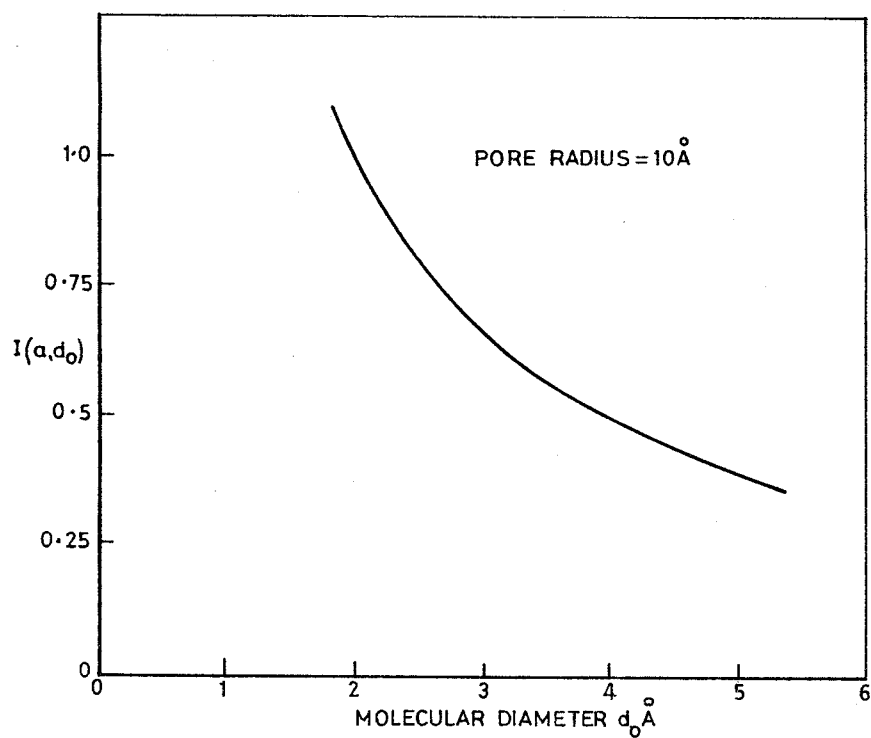
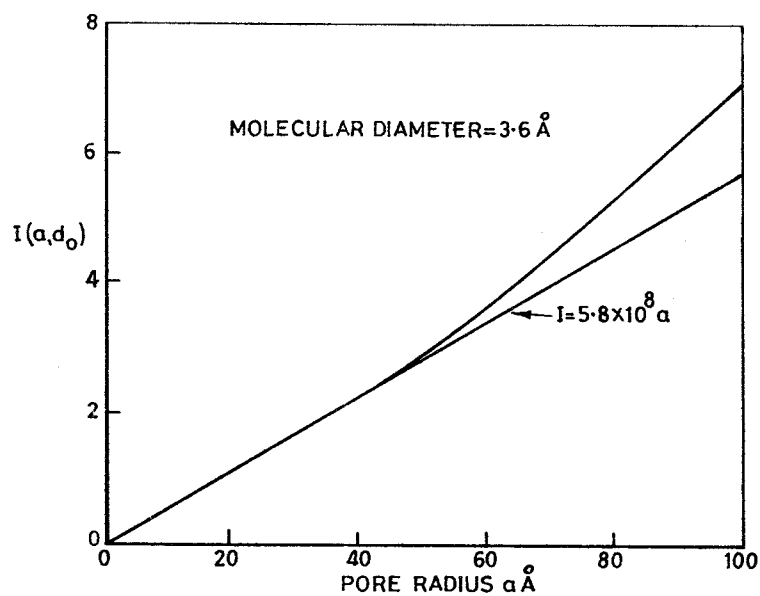


Figure 5. Interaction integral I_0 as function of y_{max}



(a)



(b)

Figure 6. Dependence of $I(a, d_0)$ a molecular diameter d_0 and pore radius a

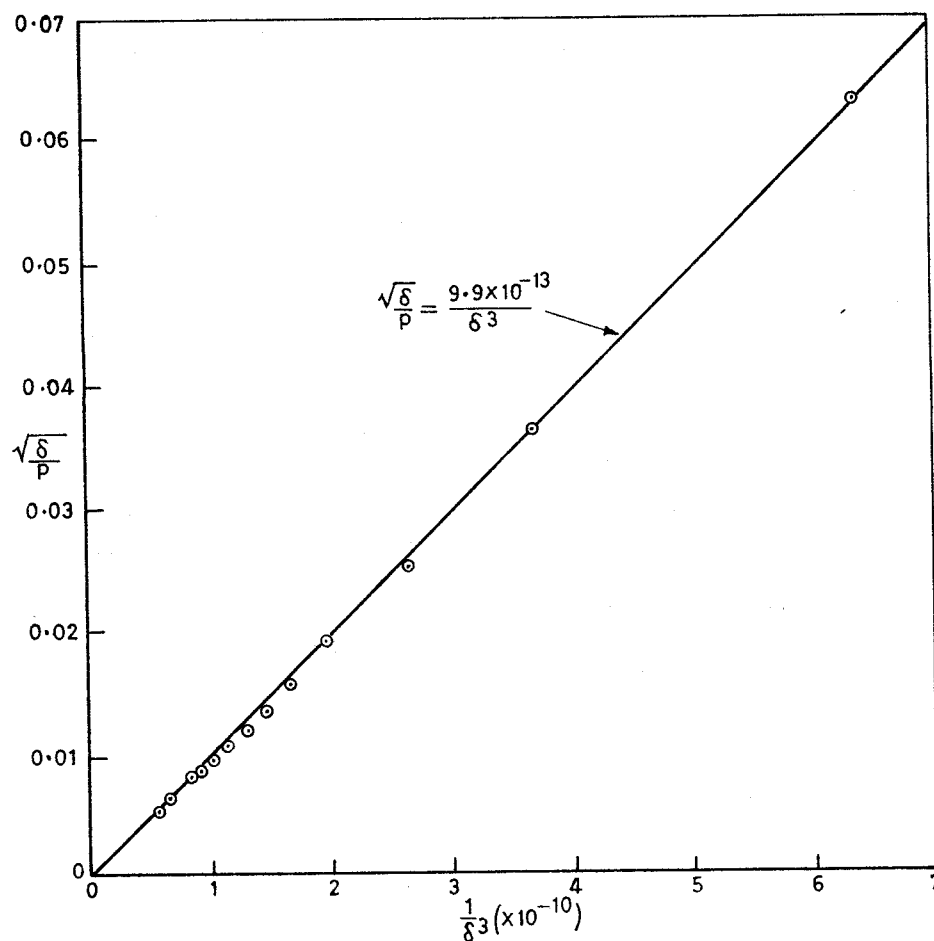


Figure 7. $\sqrt{\delta/p}$ as function of $1/\delta^3$

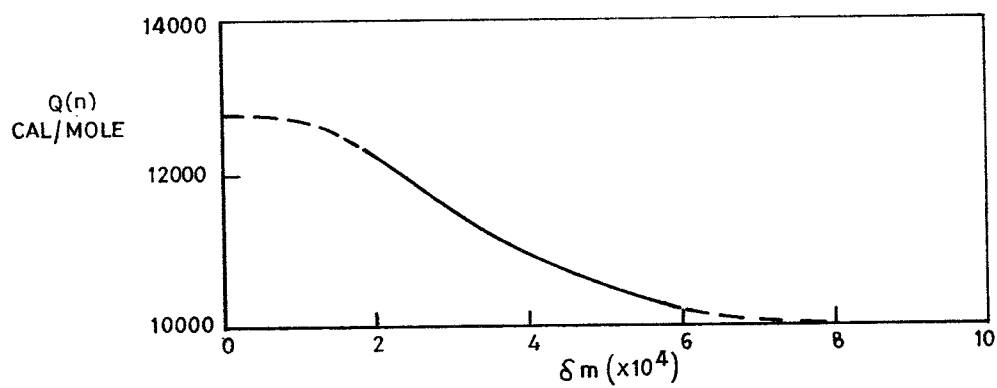


Figure 8. Mean adsorption energy as function of beam deflection

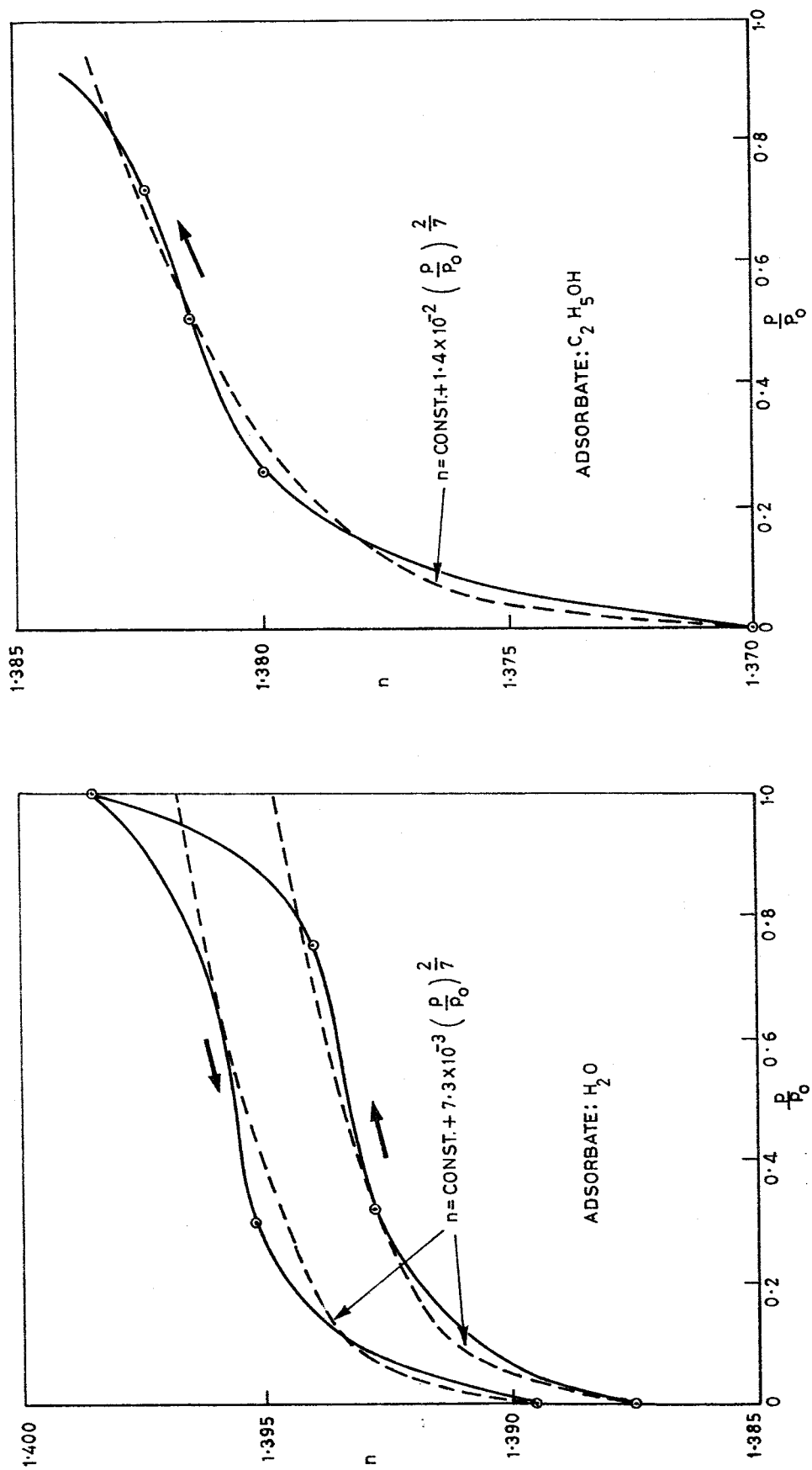


Figure 9. Effect of polar molecule adsorption on the refractive index of MgF_2

DOCUMENT CONTROL DATA SHEET

Security classification of this page

UNCLASSIFIED

1	DOCUMENT NUMBERS	2	SECURITY CLASSIFICATION
AR Number: AR-001-952		a. Complete Document: Unclassified	
Report Number: ERL-0124-TR		b. Title in Isolation: Unclassified	
Other Numbers:		c. Summary in Isolation: Unclassified	
3	TITLE STRESS IN POROUS THIN FILMS THROUGH ADSORPTION OF POLAR MOLECULES		
4	PERSONAL AUTHOR(S): E.H. Hirsch	5	DOCUMENT DATE: March 1980
		6	6.1 TOTAL NUMBER OF PAGES 20
		6.2 NUMBER OF REFERENCES: 15	
7	7.1 CORPORATE AUTHOR(S): Electronics Research Laboratory	8	REFERENCE NUMBERS a. Task: DST 79/177
7.2 DOCUMENT SERIES AND NUMBER Electronics Research Laboratory 0124-TR		b. Sponsoring Agency:	
9		9	COST CODE: 394 656
10	IMPRINT (Publishing organisation) Defence Research Centre Salisbury	11	COMPUTER PROGRAM(S) (Title(s) and language(s))
12	RELEASE LIMITATIONS (of the document): Approved for Public Release		
12.0	OVERSEAS	NO	P.R. 1 A B C D E

Security classification of this page:

UNCLASSIFIED

13 ANNOUNCEMENT LIMITATIONS (of the information on these pages):

No limitation

14 DESCRIPTORS:

a. EJC Thesaurus
Terms

Thin films	Optical coatings
Magnesium fluorides	Stability
Dipole moments	Water vapor
Electrostatics	Adsorption
Stresses	MGF2 films
Porous materials	

b. Non-Thesaurus
Terms

15 COSATI CODES:

2012

16 LIBRARY LOCATION CODES (for libraries listed in the distribution):

17 SUMMARY OR ABSTRACT:

(if this is security classified, the announcement of this report will be similarly classified)

Films of magnesium fluoride are found to be under large tensile stress following exposure to water vapour. It is shown that this stress, which varies reversibly in magnitude with the adsorption equilibrium, can be attributed to electro-static dipole interaction between the adsorbed water molecules.

The effect is not confined to magnesium fluoride, but can occur in other materials of an appropriate porous structure. Its relevance to the stability of optical coatings is discussed, together with some other applications.